Chemosphere 229 (2019) 103–111

Contents lists available at ScienceDirect

Chemosphere

journal homepage: www.elsevier.com/locate/chemosphere

Disruption of erythrocyte membrane asymmetry by triclosan is preceded by calcium dysregulation and p38 MAPK and RIP1 stimulation

Mohammad A. Alfhili [a, b], Douglas A. Weidner [c], Myon-Hee Lee [a, d, *]

[a] Department of Medicine (Division of Hematology/Oncology), Brody School of Medicine, East Carolina University, Greenville, NC 27834, United States
[b] Department of Clinical Laboratory Sciences, College of Applied Medical Sciences, King Saud University, Riyadh, 11433, Saudi Arabia
[c] Department of Microbiology & Immunology, Brody School of Medicine, East Carolina University, Greenville, NC 27834, United States
[d] Lineberger Comprehensive Cancer Center, University of North Carolina-Chapel Hill, Chapel Hill, NC 27599, United States

HIGHLIGHTS

- TCS exerts a hemolytic effect on human red blood cells.
- TCS induces eryptosis by elevated intracellular Ca^{2+} levels.
- TCS stimulates hemolysis and seryptosis at least in part through Ca^{2+} mobilization, and p38 MAPK and RIP1 activation.

ARTICLE INFO

Article history:
Received 29 January 2019
Received in revised form
22 April 2019
Accepted 28 April 2019
Available online 4 May 2019

Handling Editor: Jian-Ying Hu

Keywords:
Triclosan
Phosphatidylserine
Eryptosis
Hemolysis
p38 MAPK
RIP1

ABSTRACT

Triclosan (TCS) is a broad-spectrum antimicrobial used in personal care products, household items, and medical devices. Owing to its apoptotic potential against tumor cells, TCS has been proposed for the treatment of malignancy. A major complication of chemotherapy is anemia, which may result from direct erythrocyte hemolysis or premature cell death known as eryptosis. Similar to nucleated cells, eryptotic cells lose membrane asymmetry and Ca^{2+} regulation, and undergo oxidative stress, shrinkage, and activation of a host of kinases. In this report, we sought to examine the hemolytic and eryptotic potential of TCS and dissect the underlying mechanistic scenarios involved there in. Hemolysis was spectrophotometrically evaluated by the degree of hemoglobin release into the medium. Flow cytometry was utilized to detect phosphatidylserine (PS) exposure by annexin-V binding, intracellular Ca^{2+} by Fluo-3/AM fluorescence, and oxidative stress by 2-,7-dichlorodihydrofluorescin diacetate ($DCFH_2$-DA). Incubation of cells with 10–100 μM TCS for 1–4 h induced time- and dose-dependent hemolysis. Moreover, TCS significantly increased the percentage of eryptotic cells as evident by PS exposure (significantly enhanced annexin-V binding). Interestingly, TCS-induced eryptosis was preceded by elevated intracellular Ca^{2+} levels but was not associated with oxidative stress. Cotreatment of erythrocytes with 50 μM TCS and 50 μM SB203580 (p38 MAPK inhibitor), or 300 μM necrostatin-1 (receptor-interacting protein 1 (RIP1) inhibitor) significantly ameliorated TCS-induced PS externalization. We conclude that TCS is cytotoxic to erythrocytes by inducing hemolysis and stimulating premature death at least in part through Ca^{2+} mobilization, and p38 MAPK and RIP1 activation.

1. Introduction

Triclosan (TCS), or 5-chloro-2-(2,4-dichlorophenoxy) phenol, is a broad-spectrum antimicrobial extensively used in personal care and hygiene products, clothing and textiles, kitchenware, and medical devices (Yueh and Tukey, 2016) (Fig. 1A). A recognized endocrine disruptor, exposure to TCS may be implicated in a myriad of serious disease conditions including immune and thyroid disorders (Clayton et al., 2011). At the cellular level, TCS induces cytotoxicity, membrane damage, oxidative stress, and apoptosis (Yueh and Tukey, 2016). In particular, the antibacterial and cytotoxic effects of TCS are attributed in part to its inhibitory action on

* Corresponding author. 600 Moye Blvd, Greenville, NC 27858, United States.
E-mail address: leemy@ecu.edu (M.-H. Lee).

https://doi.org/10.1016/j.chemosphere.2019.04.211
0045-6535/

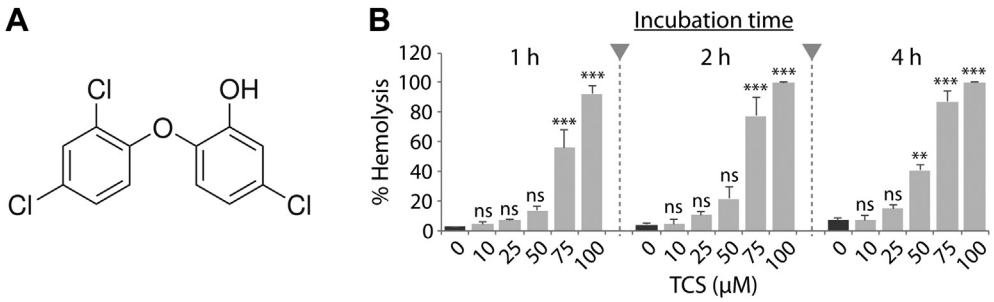

Fig. 1. TCS induces hemolysis dose and time responsively. A. Chemical structure of TCS. **B.** Arithmetic means ± SEM ($n = 9$) of RBC hemolysis following incubation for 1–4 h in Ringer solution without (black bars) or with 10–100 μM TCS (grey bars). ns indicates not significant; **($p < 0.01$) and ***($p < 0.001$) indicate significant difference from control (Student's *t*-test).

de novo fatty acid synthesis by inactivating fatty acid synthase (FAS). Because FAS is differentially upregulated in a variety of tumors (Wang et al., 2001), TCS along with other FAS inhibitors has been proposed as a promising antineoplastic agent against breast, epithelial, and prostatic cancer cells (Sadowski et al., 2014).

Owing to widespread exposure in humans, TCS has been shown to accumulate in various tissues and body fluids including the brain (up to 0.23 ng/g tissue) and blood (up to 1 μM) (Geens et al., 2012; Weatherly and Gosse, 2017). Red blood cells (RBCs), also known as erythrocytes, are highly specialized, terminally differentiated cells responsible for oxygen delivery and carriage of immune complexes. Whereas RBCs have an average lifespan of 100–120 days, various stimuli, including xenobiotics, may trigger eryptosis; the suicidal death of erythrocytes. Distinctive features of eryptotic cells include cell shrinkage, membrane blebbing, and lipid bilayer scrambling leading to phosphatidylserine (PS) externalization to the outer membrane leaflet. Adverse conditions that often precede eryptosis include energy depletion, osmotic shock, hyperthermia, and oxidative stress (Lang et al., 2012).

Accelerated eryptosis constitutes an integral part of the multifaceted pathophysiology of a plethora of diseases. These include metabolic syndrome, diabetes mellitus, anemia, renal disease, and cancer (Lang and Lang, 2015b; Lang et al., 2017). Moreover, the presence of eryptotic cells in the circulation is detrimental because they aggravate anemia and adhere to platelets and endothelial cells, giving rise to intravascular coagulation and thrombosis (Borst et al., 2012; Walker et al., 2014). Therefore, mature erythrocytes have developed an intricate and elaborate machinery to regulate survival and senescence. This regulatory network has calcium homeostasis at its core, in addition to intracellular mediators such as p38 mitogen-activated protein kinase (MAPK), caspases, AMP-activated protein kinase (AMPK), Janus kinase 3 (JAK3), and receptor-interacting protein 1 (RIP1), among others (LaRocca et al., 2014; Lang and Lang, 2015a). Cytosolic accumulation of calcium eventually leads to membrane scrambling, calpain-dependent blebbing, and cell shrinkage following KCl and water loss (Al Mamun Bhuyan et al., 2017). Similarly, eryptosis may be initiated through signaling cascades involving either the cyclooxygenase-prostaglandin E2 (COX-PGE2) pathway or the stimulation of phospholipase 2 (PLA2) and ceramide formation (Lang et al., 2012).

Despite the revitalized interest in TCS as a cause for concern (Dann and Hontela, 2011; Yueh and Tukey, 2016), and the prevalence of chemotherapy-induced anemia in cancer (Rodgers et al., 2012; Lang et al., 2017), very little emphasis has been placed on the interaction of TCS with erythrocytes. Thus, the objective of this study was to characterize the hemolytic and eryptotic potential of TCS in this cell type. It was revealed that TCS triggers premature cell death through membrane damage, evident as overt hemolysis, and loss of membrane asymmetry. Mechanistically, TCS-induced PS exposure was characterized by cytosolic Ca^{2+} accumulation along with p38 MAPK and RIP1 stimulation.

2. Materials and methods

2.1. Erythrocytes, chemicals, and solutions

Fresh, lithium heparin RBC samples from consented, healthy adults were obtained from ZenBio (Research Triangle Park, NC, USA). Samples were washed in phosphate-buffered saline (PBS; 0.9% NaCl, 1 mM KH_2PO_4, 5.6 mM Na_2HPO_4; pH 7.4) at 3000 rpm for 10 min at 21 °C, and stored in Alsever's solution at 4 °C for a maximum of 20 days (Kucherenko and Bernhardt, 2015). Samples were validated for experimentation by low (≤5%) hemolysis and PS exposure in control cells (Lupescu et al., 2014; Alfhili et al., 2019). TCS treatment was conducted *in vitro* at 5% hematocrit in Ringer solution containing: 125 mM NaCl, 5 mM KCl, 1 mM $MgSO_4$, 32 mM *N*-2-hydroxyethylpiperazine-*N*-2-ethanesulfonic acid (HEPES), 5 mM glucose, 1 mM $CaCl_2$; pH 7.4. To test for the dependence of TCS-mediated PS exposure on extracellular Ca^{2+} influx, or intracellular Ca^{2+} availability, cells were incubated in Ca^{2+}-free Ringer solution in which $CaCl_2$ was substituted with 1 mM ethylene glycol-bis(β-aminoethyl ether)-*N*,*N*,*N*′,*N*′-tetraacetic acid (EGTA) (Chem-Impex Intl., Wood Dale, IL, USA), or were cotreated with 50 μM TCS and 50 μM Ca^{2+} chelator BAPTA-AM. All chemicals were of analytical grade and were purchased from Sigma (St. Louis, MO, USA) unless otherwise noted. An ethanolic stock solution of TCS was prepared at 10 mM and diluted to desired concentrations in Ringer solution.

2.2. Hemolysis

RBCs at 5% hematocrit were exposed to 10–100 μM of TCS in Ringer solution for 1, 2, and 4 h at 37 °C. Following treatment, samples were centrifuged at 13,300 RPM for 1 min, and the degree of hemoglobin release into the medium was measured by absorbance (*A*) at 405 nm using VersaMax™ ELISA microplate reader (Molecular Devices, San Jose, CA, USA). Cells suspended in distilled water constituted 100% hemolysis, and the relative percent hemolysis was calculated according to the formula:

$$\%\,\text{Hemolysis} = (\text{As}/\text{Aw}) \times 100$$

where As = absorbance of test sample, and Aw = absorbance of positive (distilled water) control.

2.3. Detection of PS externalization and forward scatter (FSC)

Following TCS treatment, 50 μl of cells were washed in Ringer solution containing 5 mM $CaCl_2$ and resuspended in a total volume

of 200 μl. The resulting RBC suspension was stained with a 1% v/v solution of Annexin V-FITC (Thermo Fisher Scientific, Waltham, MA, USA) for 10 min at room temperature away from light. PS exposure and forward scatter FSC were subsequently determined by flow cytometry using a FACScan (Betcon Dickinson, Franklin Lakes, NJ, USA) at excitation and emission wavelengths of 488 nm and 530 nm, respectively.

2.4. Involvement of kinases

Signaling kinases were evaluated by treating the cells to a combination of 50 μM TCS and 50 μM p38 MAPK inhibitor SB203580 (Selleckchem, Houston, TX, USA), 100 μM pan-caspase inhibitor z-VAD-fmk (Selleckchem), 1 μM protein kinase C (PKC) inhibitor staurosporine (StSp; Cayman Chemical Company, Ann Arbor, MI, USA), 100 μM casein kinase 1 (CK1) inhibitor (D4476; Cayman), 300 μM RIP1 inhibitor necrostatin-1 (Nec-1), or 1 μM mixed lineage kinase domain-like (MLKL) pseudokinase inhibitor necrosulfonamide (NSA).

2.5. Confocal microscopy

Control and TCS-treated cells were stained with Annexin-V-FITC as detailed above and a homogeneous 20 μl cell suspension was spread on a glass slide before it was immediately examined with a Zeiss LSM 700 laser scanning microscope (Carl Zeiss Microscopy LLC, Thornwood, NY, USA) under a water immersion Plan-Neofluar 40/1.3 NA DIC objective.

2.6. Determination of intracellular calcium

Cytosolic Ca^{2+} activity was determined by Fluo3/AM fluorescence (Biotium, Fremont, CA, USA). The membrane-permeant Fluo3/AM ester is hydrolyzed intracellularly by esterases into Fluo3 whose fluorescence increases upon binding to Ca^{2+} ions, thus serving as an indicator of Ca^{2+} content. Following TCS treatment, 50 μl of cell suspension was washed in 5 mM $CaCl_2$ Ringer buffer and incubated with 5 μM of Fluo3/AM for 30 min at 37 °C under protection from light. Cells were washed twice to remove excess stain, resuspended in 200 μl of 5 mM $CaCl_2$ Ringer solution, and finally analyzed by a FACScan at 488 nm excitation and 530 nm emission wavelengths. The geomean of Fluo3-dependent fluorescence was subsequently determined.

2.7. Measurement of ROS generation

Oxidative stress was assayed by measuring the generation of reactive oxygen species (ROS) using the probe 2-,7-dichlorodihydrofluorescin diacetate ($DCFH_2$-DA) (Thermo Fisher Scientific, Waltham, MA, USA). $DCFH_2$-DA is a cell-permeant indicator that remains non-fluorescent until it is cleaved by intracellular esterases and in turn oxidized by ROS into the fluorescent DCF. Following treatment with 50 μM TCS, 50 μl of cell suspension was washed in Ringer buffer, resuspended in a final volume of 200 μl, and incubated with 10 μM $DCFH_2$-DA for 30 min at 37 °C in total darkness. DCF fluorescence was measured on a FACScan at excitation and emission wavelengths of 488 nm and 530 nm, respectively.

2.8. Statistical analysis

Data are shown as arithmetic means ± S.E.M. of three independent experiments conducted on RBC samples obtained from three different donors. For hemolytic assays, data were analyzed by one-way ANOVA followed by Tukey's *post hoc* test. For other experiments, student *t*-test was employed to analyze differences among the means. In all cases, a value of $P < 0.05$ was defined as the cutoff for statistical significance. *n* denotes the number of technical replicates tested. To control for individual variation and differential susceptibility to external stimuli, only control and experimental cells from the same RBC specimen were compared.

3. Results

3.1. TCS induces hemolysis time- and dose-dependently

Various xenobiotics have been shown to exhibit a hemolytic activity against human RBCs (Lang and Lang, 2015b), and the cytotoxicity of TCS was demonstrated in various cell types (Honkisz et al., 2012; Zhang et al., 2015; Park et al., 2016). To assess the hemolytic potential of TCS, erythrocytes were incubated with 10–100 μM TCS for 1, 2, and 4 h at 37 °C, and hemoglobin release into the medium was measured as a function of cell lysis relative to cells lysed in distilled water. As depicted in Fig. 1B, incubation of RBCs at the tested concentrations resulted in a dose- and time-dependent increase in hemolysis, an effect reaching statistical significance at 25 μM following 1 h exposure. This indicates that TCS exerts a hemolytic effect on RBCs that is proportionally related to length of exposure time and concentration used.

3.2. TCS causes membrane phospholipid scrambling

Previous studies have demonstrated that TCS induces apoptosis in a variety of human cell types including prostatic and placental cells (Sadowski et al., 2014; Zhang et al., 2015). In RBCs, among the distinctive features of eryptosis are PS exposure and cell shrinkage. To investigate the ability of TCS to stimulate eryptosis, RBCs were incubated in Ringer solution containing 10–50 μM TCS for 4 h at 37 °C. Cells were then stained with Annexin-V-FITC and analyzed using flow cytometry. Cell size was simultaneously estimated from FSC. Our results show that TCS increased PS externalization with a statistical significance starting at 25 μM (Fig. 2A–C). Membrane scrambling was, however, not accompanied by alterations in cell volume as indicated by the unchanged FSC under control and experimental conditions (Fig. 2D and E). Taken together, these data suggest that TCS leads to enhanced PS translocation characteristic of eryptotic cells without concurrent reduction in cell volume.

3.3. TCS disturbs calcium homeostasis

Membrane scrambling is initiated by increased activity of cytosolic Ca^{2+} (Lang et al., 2012). To test whether Ca^{2+} accumulation is precedent to PS exposure, cells were treated with 10–50 μM TCS in Ringer solution for 4 h at 37 °C, stained with Fluo3/AM, and the fluorescence intensity was analyzed by flow cytometry. It was noted that TCS treatment induced intracellular Ca^{2+} levels, an effect attaining statistical significance at 50 μM (Fig. 3).

Elevated intracellular Ca^{2+} may be due to influx into the cell through Ca^{2+}-permeable cation channels. To examine whether the increase in cytosolic Ca^{2+} was due to extracellular Ca^{2+} entry, cells were incubated with or without 50 μM TCS for 4 h at 37 °C in Ringer solution or in Ca^{2+}-free Ringer solution, and the ion's activity was estimated as described earlier. As seen in Fig. 4, Fluo3 fluorescence was not significantly altered in presence or absence of extracellular Ca^{2+}, suggesting that TCS-induced elevated cytosolic Ca^{2+} was not consequent to extracellular influx of the ion.

Next, we sought to assess the role of Ca^{2+} in TCS-mediated PS translocation. To this end, Annexin-V binding was detected in control and TCS-treated cells in presence and absence of

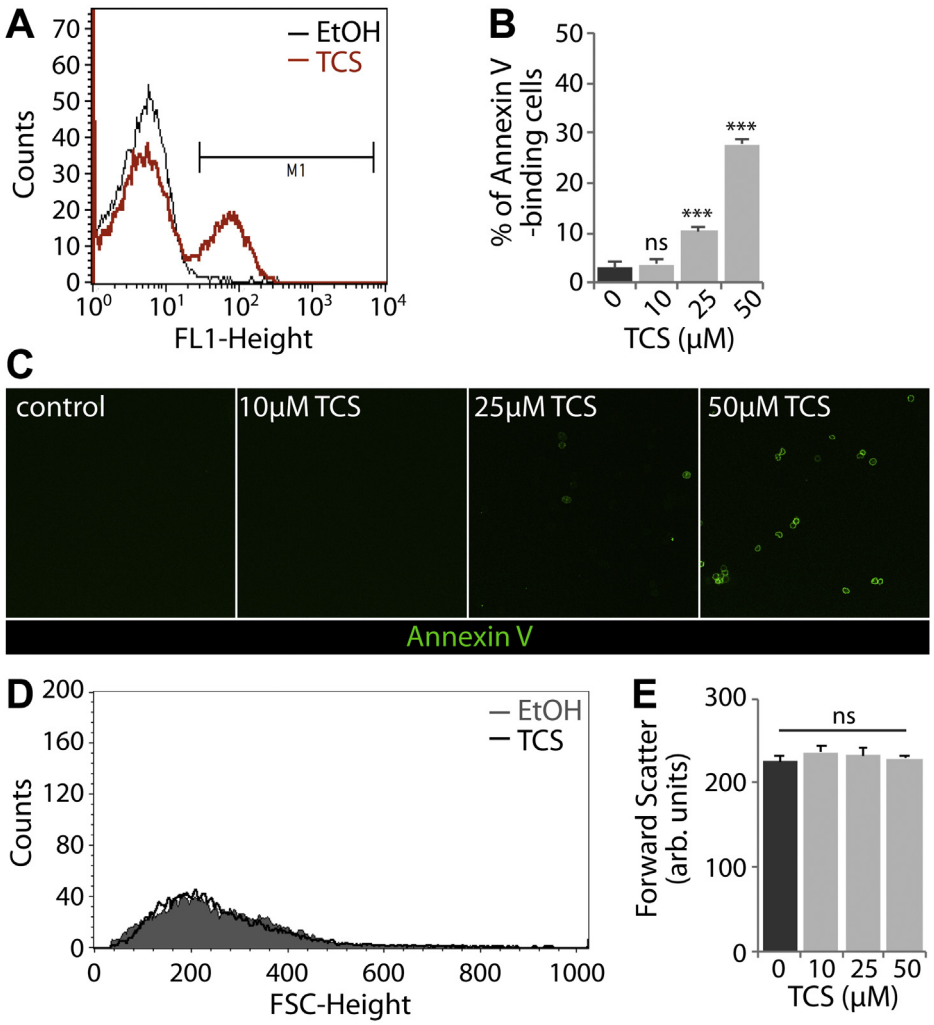

Fig. 2. Effect of TCS on phosphatidylserine exposure and forward scatter. **A.** Representative histogram showing annexin-V-binding of RBCs incubated for 4 h in Ringer solution without (black line) or with (red line) 50 μM TCS. **B.** Arithmetic means ± SEM ($n = 9$) of the percentage of annexin-V-binding RBCs following incubation for 4 h in Ringer solution without (black bar) or with 10–50 μM TCS (grey bars). **C.** Confocal microscopy images demonstrating control and eryptotic cells with increased FITC fluorescence reflective of enhanced PS exposure. **D.** Representative histogram showing erythrocyte FSC after 4 h incubation in Ringer solution without (grey peak) or with (black line) 50 μM TCS. **E.** Arithmetic means ± SEM ($n = 9$) of erythrocyte FSC after 4 h incubation without (black bar) or with 10–50 μM TCS (grey bars). ns indicates not significant; ***($p < 0.001$) indicates significant difference from control (Student's *t*-test). (For interpretation of the references to colour in this figure legend, the reader is referred to the Web version of this article.)

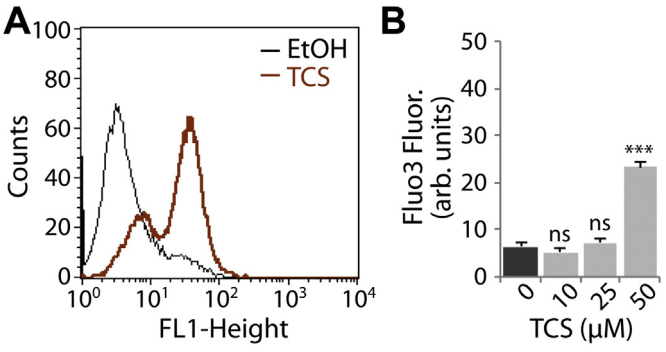

Fig. 3. TCS causes intracellular Ca^{2+} mobilization. **A.** Representative histogram showing Fluo3 fluorescence as a function of cytosolic free Ca^{2+} in RBCs incubated for 4 h in Ringer solution without (black line) or with (brown line) 50 μM TCS. **B.** Arithmetic means ± SEM ($n = 9$) of Fluo3 fluorescence in RBCs following incubation for 4 h in Ringer solution without (black bar) or with 10–50 μM TCS (grey bars). ns indicates not significant; ***($p < 0.001$) indicate significant difference from control (Student's *t*-test). (For interpretation of the references to colour in this figure legend, the reader is referred to the Web version of this article.)

extracellular Ca^{2+}, or with and without 50 μM BAPTA-AM (a selective Ca^{2+} chelator) for 4 h at 37 °C. Compared to unaltered Ca^{2+} conditions, the percentage of cells exposing PS was not significantly reduced neither when extracellular Ca^{2+} was removed (Fig. 5A–C) nor when intracellular Ca^{2+} was chelated with BAPTA-AM (Fig. 5D–F). Thus, preventing extracellular Ca^{2+} influx or depleting intracellular Ca^{2+} are apparently not required for the full PS-exposing activity of TCS.

3.4. TCS does not induce oxidative stress

The generation of excessive amounts of ROS is a recognized aggravator of eryptosis (Lang et al., 2014). We have previously shown that damage associated with TCS exposure is in part due to oxidative stress (Yoon et al., 2017). Thus, to test whether TCS-mediated PS translocation is preceded by ROS generation, cells were incubated with or without 50 μM TCS in Ringer solution for 4 h at 37 °C, and ROS levels were assessed by DCF fluorescence using flow cytometry. Fig. 6 demonstrates that ROS levels are not significantly changed by TCS treatment, suggesting that TCS-

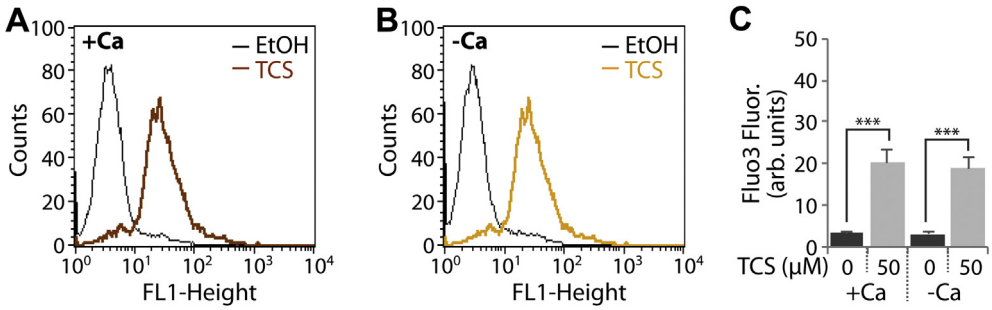

Fig. 4. Effect of extracellular Ca^{2+} chelation on TCS-induced Ca^{2+} mobilization. **A,B**. Representative histograms showing Fluo3 fluorescence as a function of cytosolic free Ca^{2+} in RBCs incubated for 4 h without (black line) or with 50 μM TCS in presence (brown line, A) and absence (yellow line, B) of extracellular Ca^{2+}. **C.** Arithmetic means ± SEM ($n = 9$) of Fluo3 fluorescence in RBCs following incubation for 4 h without (black bars) or with 50 μM TCS (grey bars) in presence or nominal absence of extracellular Ca^{2+}. ***($p < 0.001$) indicates significant difference from control (Student's *t*-test). (For interpretation of the references to colour in this figure legend, the reader is referred to the Web version of this article.)

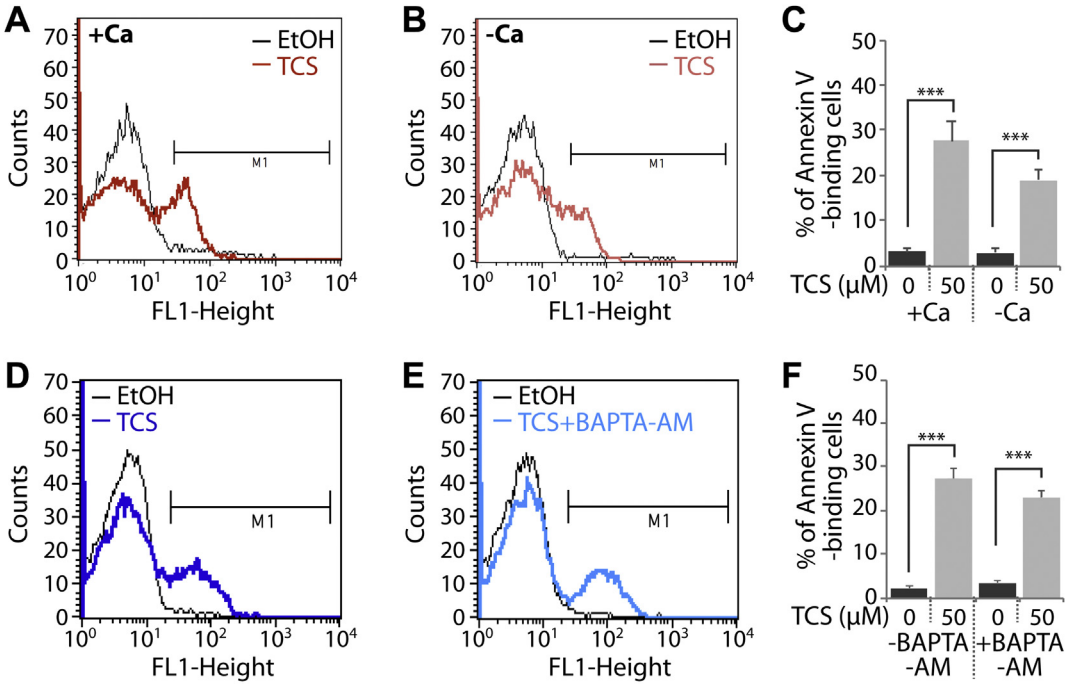

Fig. 5. Effect of extracellular Ca^{2+} chelation on TCS-induced PS exposure. **A,B**. Representative histograms showing annexin-V-binding RBCs incubated for 4 h without (black line) or with 50 μM TCS in presence (red line, A) and absence (blush line, B) of extracellular Ca^{2+}. **C.** Arithmetic means ± SEM ($n = 9$) of the percentage of annexin-V-binding cells incubated for 4 h without (black bars) or with 50 μM TCS (grey bars) in presence and absence of extracellular Ca^{2+}. **D,E**. Representative histograms showing annexin-V-binding RBCs incubated for 4 h without (black line) or with 50 μM TCS in absence (blue line, D) and presence (sky blue line, E) of 50 μM BAPTA-AM. **F.** Arithmetic means ± SEM ($n = 9$) of the percentage of annexin-V-binding cells incubated for 4 h without (black bars) or with 50 μM TCS (grey bars) in absence and presence of 50 μM BAPTA-AM. ***($p < 0.001$) indicates significant difference from control (Student's *t*-test). (For interpretation of the references to colour in this figure legend, the reader is referred to the Web version of this article.)

induced eryptosis is not mediated through oxidative stress.

3.5. Involvement of kinases

Multiple signaling pathways have been implicated in eryptosis, including p38 MAPK, caspases, PKC, and CK1 (Lang and Lang, 2015a). RIP1 and MLKL have also been recently described, revealing necroptosis as a distinct death pathway in RBCs (LaRocca et al., 2014). To identify kinases stimulated in response to TCS exposure, cells were incubated in Ringer solution with or without 50 μM TCS in presence and absence of 50 μM SB203580 (p38 MAPK inhibitor), 100 μM zVAD-fmk (pan-caspase inhibitor), 1 μM StSp (PKC inhibitor), 100 μM D4476 (CK1 inhibitor), 300 μM Nec-1 (RIP1 inhibitor), or 1 μM NSA (MLKL inhibitor) for 4 h at 37 °C. PS translocation was subsequently evaluated as previously described. As seen in Fig. 7, both SB203580 and Nec-1 significantly but not thoroughly blunted PS translocation, while no statistically significant inhibition was observed under caspase, PKC, CK1, or MLKL blockage. This identifies p38 MAPK and RIP1 not only as molecular targets of TCS, but also as essential requirements for its full eryptotic activity.

4. Discussion

TCS is a high-volume, antimicrobial phenolic compound commonly used as a preservative in personal care products, textiles, medical devices, and food contact materials (Nietch et al., 2013; Yueh and Tukey, 2016). Once absorbed, TCS is distributed and deposited in a variety of tissues and body fluids, including the liver, brain, and blood. Toxicological profiling of TCS has discerned

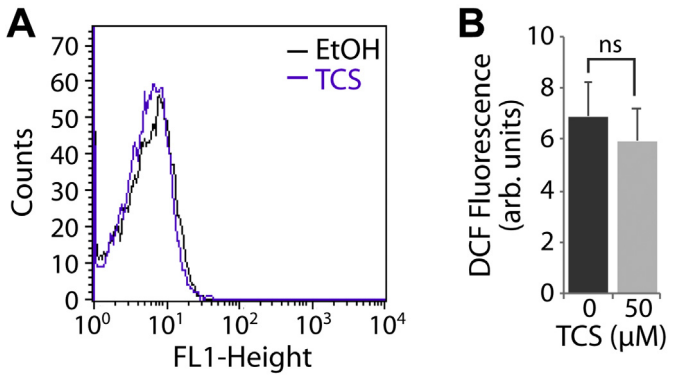

Fig. 6. Effect of TCS on ROS levels. A. Representative histogram showing DCF fluorescence after 4 h incubation in Ringer solution without (black line) or with (purple line) 50 μM TCS. **B.** Arithmetic means ± SEM ($n = 9$) of DCF geomean fluorescence after 4 h incubation without (black bar) or with 50 μM TCS (grey bar). ns indicates not significant. (For interpretation of the references to colour in this figure legend, the reader is referred to the Web version of this article.)

its apoptotic potency in a variety of tumor cells, which could be exploited for therapeutic purposes. Thus, complementary to previous studies, this work not only expands on current understanding of TCS toxicity, but also offers assessment of its therapeutic potential as an anticancer agent. It is worth mentioning that pathogens whose tropism involves the RBC are highly likely to transform infected cells into eryptotic corpses, as is the case with *Plasmodium spp.* (Foller et al., 2009). Thus, elucidating the effects of TCS on RBCs becomes more relevant considering that, in addition to its antimalarial properties, TCS is known to be effective against important hemoparasites, including *Babesia*, *Trypanosoma*, *Leishmania*, and *Toxoplasma* (Bork et al., 2003; Roberts et al., 2003; Otero et al., 2014).

To the best of our knowledge, this is the first study to report that TCS stimulates eryptosis; the suicidal erythrocyte death. TCS elicited hemolysis and eryptosis in micromolar concentrations that are lower than the millimolar levels present in consumer products (3.5–17 mM) (Weatherly and Gosse, 2017), and which are within the range shown to possess antitumor activity (10–350 μM) (Deepa et al., 2012; Winitthana et al., 2014). It is important to keep in mind that TCS adverse effects described herein are based on RBCs obtained from healthy individuals. Such findings may parallel effects of lower doses in RBCs from cancer patients considering the augmented susceptibility of those cells to eryptosis (Lang et al., 2017). Pending *in vivo* confirmation, data from this exploratory

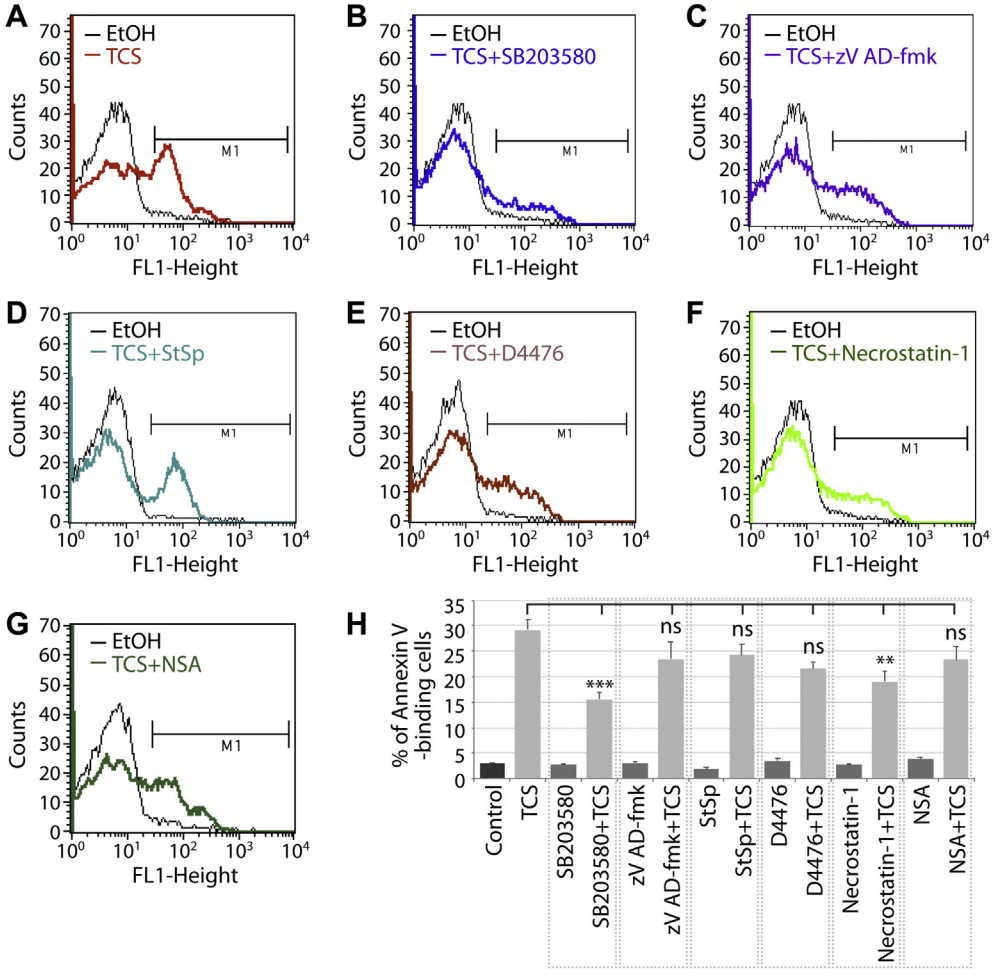

Fig. 7. TCS-induced phosphatidylserine exposure is suppressed by SB203580 and necrostatin-1. A-G Representative histograms showing annexin-V-binding RBCs incubated for 4 h without (black line) or with 50 μM TCS in absence (red line, A) and presence of 50 μM SB203580 (blue line, B), 100 μM zVAD-fmk (purple line, C), 1 μM StSp (turquoise line, D), 100 μM D4476 (brown line, E), 300 μM necrostatin-1 (lime line, F), or 1 μM NSA (green line, G). **H.** Arithmetic means ± SEM ($n = 9$) of the percentage of annexin-V-binding cells incubated for 4 h in Ringer solution without (black bar) or with 50 μM TCS (grey bars) in absence and presence of 50 μM SB203580, 100 μM zVAD-fmk, 1 μM StSp, 100 μM D4476, 300 μM Nec-1, or 1 μM NSA. ns indicates not significant; **($p < 0.01$) and ***($p < 0.001$) indicate significant difference from TCS-only cells (Student's *t*-test). (For interpretation of the references to colour in this figure legend, the reader is referred to the Web version of this article.)

study provides evidence of a novel eryptotic sequela of TCS that may warrant careful consideration of its use for chemotherapy.

Similar to findings reported by Miller et al. (Miller and Deinzer, 1980), TCS was shown to be highly toxic to erythrocytes causing conspicuous hemolysis indicative of direct membrane damage. The lack of ROS generation seems to rule out oxidative stress as a contributing factor in TCS-induced hemolysis, as was observed for *para*-hydroxyanisole, and in contrast to bisphenol A (BPA), two related phenolic compounds (Nohl and Stolze, 1998; Macczak et al., 2016; Sicinska, 2018). Circulating, naked hemoglobin is highly reactive and can participate in oxidative damage manifested as perturbations in endothelial cell function, hypertension, thrombosis, and atherosclerotic lesions (Miller and Shaklai, 1999; Reiter et al., 2002; Studt et al., 2005; Silva et al., 2009). Similarly, extravascular presence of free hemoglobin is associated with dysregulated iron homeostasis, renal tubular injury, and neuronal damage (Tracz et al., 2007; Lara et al., 2009; Pantopoulos et al., 2012).

Our data also show that TCS causes a significant increase in eryptotic cells as detected by PS externalization, which is in congruence with its apoptotic activity observed in nucleated cells (Deepa et al., 2012; Honkisz et al., 2012; Szychowski et al., 2016). Several other compounds structurally related to TCS, such as BPA and chlorophenols, have recently been shown to also trigger eryptosis (Macczak et al., 2016; Michalowicz et al., 2018; Jarosiewicz et al., 2019). Under physiological conditions, eryptosis may be perceived as a counterpoise to erythropoiesis, preventing both anemia and polycythemia. This is because exposure of PS serves as a conserved flag on RBCs undergoing eryptosis for recognition and removal by the monocyte-macrophage system (Lang et al., 2003), thus acting as a safeguard against hemolysis.

Inordinate eryptosis constitutes a common theme in a variety of life-threatening conditions including diabetes, hepatic failure, and malignancy (Lang and Lang, 2015a). In these cases and many others, eryptotic cells may adhere to endothelial cells and platelets, obstruct microcirculatory flow, and lead to thrombosis (Borst et al., 2012; Walker et al., 2014). This is a consequence of the negative impact the eryptotic RBC membrane exerts on the cell's deformability and aggregability. When RBCs form larger aggregates with rigid membranes, blood viscosity increases, causing enhanced flow resistance, and eventually diminished tissue perfusion (du Plooy et al., 2018; Pretorius, 2018). The limited elasticity characteristic of eryptotic membranes may also hinder the cell's ability to reassume its original biconcave shape following passage through the microvasculature (Pretorius, 2018). Therefore, identifying the impact of xenobiotics on RBC rheology is among the most important aspects of pharmaceutical assessment of potential therapies.

The importance of Ca^{2+} activity in mediating eryptosis cannot be overstated, and the process has been referred to in the literature as "Ca^{2+}-dependent" programmed cell death (LaRocca et al., 2014). Activated K^+ channels in response to increased cytosolic Ca^{2+} lead to K^+ efflux, membrane hyperpolarization causing Cl^- outflow, dehydration due to water loss, and eventual cell shrinkage (Lang et al., 2012). Although TCS has been shown to cause K^+ efflux prior to hemolysis (Miller and Deinzer, 1980), we observed no significant change in cell volume among healthy and eryptotic cells despite a significant increase in intracellular Ca^{2+}. Likewise, the ionophoric effect of clofazimine was not accompanied by cell shrinkage (Officioso et al., 2015).

Because both scramblase and flippase are Ca^{2+}-sensitive, perturbations in the ion's activity are associated with loss of membrane asymmetry (Lang et al., 2006). In our study, we noted that TCS was able to cause membrane phospholipid scrambling with a significant increase in cytosolic Ca^{2+} at 50 μM. This is in consonance with recent findings demonstrating Ca^{2+} dysregulation caused by TCS both *in vitro* and *in vivo* (Ahn et al., 2008; Cherednichenko et al., 2012; Popova et al., 2018). Our data also indicate that neither PS exposure nor cytosolic Ca^{2+} was significantly blunted by Ca^{2+} depletion, underlining the dispensability of the ion in TCS-mediated eryptosis, and pointing at possible additional mechanisms. Similar findings were recently reported by Gao et al. for betulinic acid (Gao et al., 2014). Presumably, due to their hydrophobicity, both TCS and betulinic acid may readily permeabilize through the membrane to exert their effects (Guillen et al., 2004). On the other hand, some xenobiotics such as regorafenib rather depleted intracellular Ca^{2+} while still inducing eryptosis (Zierle et al., 2016). It is important to note that the use of EDTA to chelate Ca^{2+} does not provide total elimination of the ion, which must be taken into consideration when evaluating the contribution of extracellular Ca^{2+} (Al Mamun Bhuyan et al., 2017).

In RBCs, oxidative stress participates in Ca^{2+} entry by opening cation channels in the cell membrane. We have previously shown that TCS perturbs the antioxidant response in human mesenchymal stem cells (Yoon et al., 2017), and oxidative damage by TCS has been detected in a variety of cell types (Ma et al., 2013; Szychowski et al., 2016). Nevertheless, we found that TCS-induced eryptosis was not accompanied by changes in ROS levels. Interestingly, other compounds such as carnosic acid, perifosine, and micafungin rather diminished ROS production as part of their eryptotic manifestations (Stockinger et al., 2015; Peter et al., 2016; Egler and Lang, 2017). It is comprehensible to surmise that such an event is reflective of a suppressed metabolic rate and cellular adaptivity, which is compatible with the anti-inflammatory role of TCS (Barros et al., 2010).

The use of small-molecule inhibitors has allowed us to reveal the identity of molecular mediators targeted by TCS in erythrocytes. We observed that TCS-induced PS exposure was significantly inhibited by blockade of either p38 MAPK or RIP1. Inhibition of caspases, PKC, and CK1 provided some degree of protection against PS externalization, the extent of which, however, failed to attain statistical significance. p38 MAPK is an enzyme that regulates proliferation, differentiation, and apoptosis in nucleated cells (Lee et al., 2003; Cuadrado and Nebreda, 2010). Gene-targeting *in vivo* studies also suggest that p38 possesses pro-inflammatory and antitumor roles, and is therefore of interest as a pharmaceutical target (Cuadrado and Nebreda, 2010). In RBCs, p38 similarly regulates eryptosis and the osmotic response, and may be activated prior to Ca^{2+} accumulation (Gatidis et al., 2011). Most recently, Zhang et al. demonstrated that TCS promotes p38 phosphorylation *in vitro* and *in vivo* (Zhang et al., 2018), which is in accord to reports of TCS-induced p38 activation in Raw264.7 macrophages (Wang et al., 2018), and rat neural stem cells (Park et al., 2016).

Whereas p38 is a major orchestrator of eryptosis, RIP1 is known to be critical for caspase-independent cell death (Weinlich et al., 2017). Once the cell has committed to necroptosis, RIP1 forms the necrosome; a ternary complex with RIP3 and MLKL, although RIP1-independent necroptosis has also been recognized (Weinlich et al., 2017). RIP1 also signals for apoptosis, especially under inhibition of cellular inhibitor of apoptosis proteins (cIAPs), and may act upstream of p38 (Lee et al., 2003; Christofferson et al., 2014). Moreover, RIP1 has been shown to be essential for lymphocyte survival, and *Rip1*$^{-/-}$ cells are highly sensitive to apoptosis (Christofferson et al., 2014). Importantly, as is the case with p38, RIP1 is also implicated in inflammation and metastasis, identifying the enzyme as a possible therapeutic target (Weinlich et al., 2017). The existence of RIP1 and MLKL in RBCs was identified when the cells were challenged with bacterial toxins (LaRocca et al., 2014), establishing necroptosis as a mode of cell death in erythrocytes. However, because RIP1 may be involved in apoptosis and necroptosis, we were prompted to probe the involvement of the necroptosis executioner, MLKL, in TCS-induced RBC death. The results (Fig. 7G

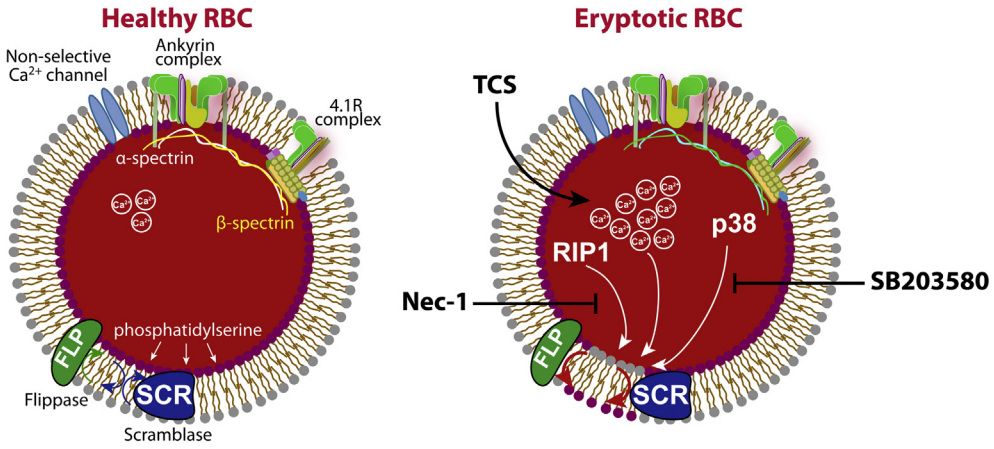

Fig. 8. A working model for TCS-induced premature erythrocyte death: TCS causes calcium ion dysregulation resulting in elevated intracellular Ca^{2+} activity. Stimulation of p38 MAPK and RIP1 signaling in response to TCS culminates in phosphatidylserine translocation to the outer membrane leaflet; an event significantly abrogated by pharmacological interference with either enzyme.

and H) demonstrated a lack of significant reduction in PS externalization under MLKL inhibition, thus possibly exonerating necroptosis as a mode of cell death. Notably, both pathways were recently found to be activated in HepG2 cells in response to Tanshinone IIA, a component of the red sage plant *Salvia miltiorrhiza* (Lin et al., 2016), which also possesses eryptotic activity (Zelenak et al., 2012).

In conclusion, this report shows that TCS adversely affects the physiology and survival of RBCs by triggering premature cell death. It was revealed that the integrity of the RBC membrane is perturbed by TCS leading to phospholipid scrambling at least in part through loss of Ca^{2+} homeostasis and p38 MAPK- and RIP1-mediated mechanisms (Fig. 8).

Competing interests

The authors declare they have no competing interests relevant to this manuscript.

Acknowledgements

We thank the members of the Lee laboratory for helpful advice and discussion during this work. This work was supported in part by the Brody Brothers Grant (216102-664261) to M-H.L. and the Saudi Government Graduate Scholarship (from King Saud University) to M.A.A.

References

Ahn, K.C., Zhao, B., Chen, J., Cherednichenko, G., Sanmarti, E., Denison, M.S., Lasley, B., Pessah, I.N., Kultz, D., Chang, D.P., Gee, S.J., Hammock, B.D., 2008. In vitro biologic activities of the antimicrobials triclocarban, its analogs, and triclosan in bioassay screens: receptor-based bioassay screens. Environ. Health Perspect. 116, 1203–1210.

Al Mamun Bhuyan, A., Nussle, S., Cao, H., Zhang, S., Lang, F., 2017. Simvastatin, a novel stimulator of eryptosis, the suicidal erythrocyte death. Cell. Physiol. Biochem. : Int. J. Exp. Cell. Physiol., Biochem, and Pharma. 43, 492–506.

Alfhili, M.A., Nkany, M.B., Weidner, D.A., Lee, M.H., 2019. Stimulation of eryptosis by broad-spectrum insect repellent N,N-Diethyl-3-methylbenzamide (DEET). Toxicol. Appl. Pharmacol. 370, 36–43.

Barros, S.P., Wirojchanasak, S., Barrow, D.A., Panagakos, F.S., Devizio, W., Offenbacher, S., 2010. Triclosan inhibition of acute and chronic inflammatory gene pathways. J. Clin. Periodontol. 37, 412–418.

Bork, S., Yokoyama, N., Matsuo, T., Claveria, F.G., Fujisaki, K., Igarashi, I., 2003. Growth inhibitory effect of triclosan on equine and bovine Babesia parasites. Am. J. Trop. Med. Hyg. 68, 334–340.

Borst, O., Abed, M., Alesutan, I., Towhid, S.T., Qadri, S.M., Foller, M., Gawaz, M., Lang, F., 2012. Dynamic adhesion of eryptotic erythrocytes to endothelial cells via CXCL16/SR-PSOX. Am. J. Physiol. Cell Physiol. 302, C644–C651.

Cherednichenko, G., Zhang, R., Bannister, R.A., Timofeyev, V., Li, N., Fritsch, E.B., Feng, W., Barrientos, G.C., Schebb, N.H., Hammock, B.D., Beam, K.G., Chiamvimonvat, N., Pessah, I.N., 2012. Triclosan impairs excitation-contraction coupling and Ca2+ dynamics in striated muscle. In: Proceedings of the National Academy of Sciences of the United States of America, 109, pp. 14158–14163.

Christofferson, D.E., Li, Y., Yuan, J., 2014. Control of life-or-death decisions by RIP1 kinase. Annu. Rev. Physiol. 76, 129–150.

Clayton, E.M., Todd, M., Dowd, J.B., Aiello, A.E., 2011. The impact of bisphenol A and triclosan on immune parameters in the U.S. population, NHANES 2003-2006. Environ. Health Perspect. 119, 390–396.

Cuadrado, A., Nebreda, A.R., 2010. Mechanisms and functions of p38 MAPK signalling. Biochem. J. 429, 403–417.

Dann, A.B., Hontela, A., 2011. Triclosan: environmental exposure, toxicity and mechanisms of action. JAT (J. Appl. Toxicol.) : JAT 31, 285–311.

Deepa, P.R., Vandhana, S., Jayanthi, U., Krishnakumar, S., 2012. Therapeutic and toxicologic evaluation of anti-lipogenic agents in cancer cells compared with non-neoplastic cells. Basic Clin. Pharmacol. Toxicol. 110, 494–503.

du Plooy, J.N., Bester, J., Pretorius, E., 2018. Eryptosis in haemochromatosis: implications for rheology. Clin. Hemorheol. Microcirc. 69, 457–469.

Egler, J., Lang, F., 2017. Triggering of eryptosis, the suicidal erythrocyte death, by perifosine. Cell. Physiol. Biochem.: Int. J. Exp. Cell. Physiol., Biochem, and Pharma. 41, 2534–2544.

Foller, M., Bobbala, D., Koka, S., Huber, S.M., Gulbins, E., Lang, F., 2009. Suicide for survival-death of infected erythrocytes as a host mechanism to survive malaria. Cell. Physiol. Biochem.: Int. J. Exp. Cell. Physiol., Biochem, and Pharma. 24, 133–140.

Gao, M., Lau, P.M., Kong, S.K., 2014. Mitochondrial toxin betulinic acid induces in vitro eryptosis in human red blood cells through membrane permeabilization. Arch. Toxicol. 88, 755–768.

Gatidis, S., Zelenak, C., Fajol, A., Lang, E., Jilani, K., Michael, D., Qadri, S.M., Lang, F., 2011. p38 MAPK activation and function following osmotic shock of erythrocytes. Cell. Physiol. Biochem.: Int. J. Exp. Cell. Physiol., Biochem, and Pharma. 28, 1279–1286.

Geens, T., Neels, H., Covaci, A., 2012. Distribution of bisphenol-A, triclosan and n-nonylphenol in human adipose tissue, liver and brain. Chemosphere 87, 796–802.

Guillen, J., Bernabeu, A., Shapiro, S., Villalain, J., 2004. Location and orientation of Triclosan in phospholipid model membranes. Eur. Biophys. J. 33, 448–453.

Honkisz, E., Zieba-Przybylska, D., Wojtowicz, A.K., 2012. The effect of triclosan on hormone secretion and viability of human choriocarcinoma JEG-3 cells. Reprod. Toxicol. 34, 385–392.

Jarosiewicz, M., Michalowicz, J., Bukowska, B., 2019. In vitro assessment of eryptotic potential of tetrabromobisphenol A and other bromophenolic flame retardants. Chemosphere 215, 404–412.

Kucherenko, Y.V., Bernhardt, I., 2015. Natural antioxidants improve red blood cell "survival" in non-leukoreduced blood samples. Cell. Physiol. Biochem.: Int. J. Exp. Cell. Physiol., Biochem, and Pharma. 35, 2055–2068.

Lang, E., Bissinger, R., Qadri, S.M., Lang, F., 2017. Suicidal death of erythrocytes in cancer and its chemotherapy: a potential target in the treatment of tumor-associated anemia. Int. J. Cancer 141, 1522–1528.

Lang, E., Lang, F., 2015a. Mechanisms and pathophysiological significance of eryptosis, the suicidal erythrocyte death. Semin. Cell Dev. Biol. 39, 35–42.

Lang, E., Lang, F., 2015b. Triggers, inhibitors, mechanisms, and significance of eryptosis: the suicidal erythrocyte death. BioMed Res. Int. 2015, 513518.

Lang, E., Qadri, S.M., Lang, F., 2012. Killing me softly - suicidal erythrocyte death. Int.

J. Biochem. Cell Biol. 44, 1236–1243.
Lang, F., Abed, M., Lang, E., Foller, M., 2014. Oxidative stress and suicidal erythrocyte death. Antioxidants Redox Signal. 21, 138–153.
Lang, F., Lang, K.S., Lang, P.A., Huber, S.M., Wieder, T., 2006. Mechanisms and significance of eryptosis. Antioxidants Redox Signal. 8, 1183–1192.
Lang, P.A., Kaiser, S., Myssina, S., Wieder, T., Lang, F., Huber, S.M., 2003. Role of Ca^{2+}-activated K^+ channels in human erythrocyte apoptosis. Am. J. Physiol. Cell Physiol. 285, C1553–C1560.
Lara, F.A., Kahn, S.A., da Fonseca, A.C., Bahia, C.P., Pinho, J.P., Graca-Souza, A.V., Houzel, J.C., de Oliveira, P.L., Moura-Neto, V., Oliveira, M.F., 2009. On the fate of extracellular hemoglobin and heme in brain. J. Cereb. Blood Flow Metab.: Off. J. Int. Soc. Cereb. Blood Flow Metab. 29, 1109–1120.
LaRocca, T.J., Stivison, E.A., Hod, E.A., Spitalnik, S.L., Cowan, P.J., Randis, T.M., Ratner, A.J., 2014. Human-specific bacterial pore-forming toxins induce programmed necrosis in erythrocytes. MBio 5 e01251-01214.
Lee, T.H., Huang, Q., Oikemus, S., Shank, J., Ventura, J.J., Cusson, N., Vaillancourt, R.R., Su, B., Davis, R.J., Kelliher, M.A., 2003. The death domain kinase RIP1 is essential for tumor necrosis factor alpha signaling to p38 mitogen-activated protein kinase. Mol. Cell Biol. 23, 8377–8385.
Lin, C.Y., Chang, T.W., Hsieh, W.H., Hung, M.C., Lin, I.H., Lai, S.C., Tzeng, Y.J., 2016. Simultaneous induction of apoptosis and necroptosis by Tanshinone IIA in human hepatocellular carcinoma HepG2 cells. Cell death discovery 2, 16065.
Lupescu, A., Bissinger, R., Warsi, J., Jilani, K., Lang, F., 2014. Stimulation of erythrocyte cell membrane scrambling by gedunin. Cell. Physiol. Biochem.: Int. J. Exp. Cell. Physiol., Biochem, and Pharma. 33, 1838–1848.
Ma, H., Zheng, L., Li, Y., Pan, S., Hu, J., Yu, Z., Zhang, G., Sheng, G., Fu, J., 2013. Triclosan reduces the levels of global DNA methylation in HepG2 cells. Chemosphere 90, 1023–1029.
Macczak, A., Cyrkler, M., Bukowska, B., Michalowicz, J., 2016. Eryptosis-inducing activity of bisphenol A and its analogs in human red blood cells (in vitro study). J. Hazard Mater. 307, 328–335.
Michalowicz, J., Wluka, A., Cyrkler, M., Macczak, A., Sicinska, P., Mokra, K., 2018. Phenol and chlorinated phenols exhibit different apoptotic potential in human red blood cells (in vitro study). Environ. Toxicol. Pharmacol. 61, 95–101.
Miller, T.L., Deinzer, M.L., 1980. Effects of nonachloropredioxin and other hydroxychlorodiphenyl ethers on biological membranes. J. Toxicol. Environ. Health 6, 11–25.
Miller, Y.I., Shaklai, N., 1999. Kinetics of hemin distribution in plasma reveals its role in lipoprotein oxidation. Biochim. Biophys. Acta 1454, 153–164.
Nietch, C.T., Quinlan, E.L., Lazorchak, J.M., Impellitteri, C.A., Raikow, D., Walters, D., 2013. Effects of a chronic lower range of triclosan exposure on a stream mesocosm community. Environ. Toxicol. Chem. 32, 2874–2887.
Nohl, H., Stolze, K., 1998. The effects of xenobiotics on erythrocytes. Gen. Pharmacol. 31, 343–347.
Officioso, A., Alzoubi, K., Manna, C., Lang, F., 2015. Clofazimine induced suicidal death of human erythrocytes. Cell. Physiol. Biochem.: Int. J. Exp. Cell. Physiol., Biochem, and Pharma. 37, 331–341.
Otero, E., Vergara, S., Robledo, S.M., Cardona, W., Carda, M., Velez, I.D., Rojas, C., Otalvaro, F., 2014. Synthesis, leishmanicidal and cytotoxic activity of triclosan-chalcone, triclosan-chromone and triclosan-coumarin hybrids. Molecules 19, 13251–13266.
Pantopoulos, K., Porwal, S.K., Tartakoff, A., Devireddy, L., 2012. Mechanisms of mammalian iron homeostasis. Biochemistry 51, 5705–5724.
Park, B.K., Gonzales, E.L., Yang, S.M., Bang, M., Choi, C.S., Shin, C.Y., 2016. Effects of triclosan on neural stem cell viability and survival. Biomolecules & therapeutics 24, 99–107.
Peter, T., Bissinger, R., Signoretto, E., Mack, A.F., Lang, F., 2016. Micafungin-induced suicidal erythrocyte death. Cell. Physiol. Biochem.: Int. J. Exp. Cell. Physiol., Biochem, and Pharma. 39, 584–595.
Popova, L.B., Nosikova, E.S., Kotova, E.A., Tarasova, E.O., Nazarov, P.A., Khailova, L.S., Balezina, O.P., Antonenko, Y.N., 2018. Protonophoric action of triclosan causes calcium efflux from mitochondria, plasma membrane depolarization and bursts of miniature end-plate potentials. Biochim. Biophys. Acta 1860, 1000–1007.
Pretorius, E., 2018. Erythrocyte deformability and eryptosis during inflammation, and impaired blood rheology. Clin. Hemorheol. Microcirc. 69, 545–550.
Reiter, C.D., Wang, X., Tanus-Santos, J.E., Hogg, N., Cannon 3rd, R.O., Schechter, A.N., Gladwin, M.T., 2002. Cell-free hemoglobin limits nitric oxide bioavailability in sickle-cell disease. Nat. Med. 8, 1383–1389.
Roberts, C.W., McLeod, R., Rice, D.W., Ginger, M., Chance, M.L., Goad, L.J., 2003. Fatty acid and sterol metabolism: potential antimicrobial targets in apicomplexan and trypanosomatid parasitic protozoa. Mol. Biochem. Parasitol. 126, 129–142.
Rodgers 3rd, G.M., Becker, P.S., Blinder, M., Cella, D., Chanan-Khan, A., Cleeland, C., Coccia, P.F., Djulbegovic, B., Gilreath, J.A., Kraut, E.H., Matulonis, U.A., Millenson, M.M., Reinke, D., Rosenthal, J., Schwartz, R.N., Soff, G., Stein, R.S., Vlahovic, G., Weir 3rd, A.B., 2012. Cancer- and chemotherapy-induced anemia. J. Natl. Compr. Cancer Netw.: J. Natl. Compr. Cancer Netw. 10, 628–653.
Sadowski, M.C., Pouwer, R.H., Gunter, J.H., Lubik, A.A., Quinn, R.J., Nelson, C.C., 2014. The fatty acid synthase inhibitor triclosan: repurposing an anti-microbial agent for targeting prostate cancer. Oncotarget 5, 9362–9381.
Sicinska, P., 2018. Di-n-butyl phthalate, butylbenzyl phthalate and their metabolites induce haemolysis and eryptosis in human erythrocytes. Chemosphere 203, 44–53.
Silva, G., Jeney, V., Chora, A., Larsen, R., Balla, J., Soares, M.P., 2009. Oxidized hemoglobin is an endogenous proinflammatory agonist that targets vascular endothelial cells. J. Biol. Chem. 284, 29582–29595.
Stockinger, K., Bissinger, R., Bouguerra, G., Abbes, S., Lang, F., 2015. Enhanced eryptosis following exposure to carnosic acid. Cell. Physiol. Biochem.: Int. J. Exp. Cell. Physiol., Biochem, and Pharma. 37, 1779–1791.
Studt, J.D., Kremer Hovinga, J.A., Antoine, G., Hermann, M., Rieger, M., Scheiflinger, F., Lammle, B., 2005. Fatal congenital thrombotic thrombocytopenic purpura with apparent ADAMTS13 inhibitor: in vitro inhibition of ADAMTS13 activity by hemoglobin. Blood 105, 542–544.
Szychowski, K.A., Wnuk, A., Kajta, M., Wojtowicz, A.K., 2016. Triclosan activates aryl hydrocarbon receptor (AhR)-dependent apoptosis and affects Cyp1a1 and Cyp1b1 expression in mouse neocortical neurons. Environ. Res. 151, 106–114.
Tracz, M.J., Alam, J., Nath, K.A., 2007. Physiology and pathophysiology of heme: implications for kidney disease. J. Am. Soc. Nephrol. 18, 414–420.
Walker, B., Towhid, S.T., Schmid, E., Hoffmann, S.M., Abed, M., Munzer, P., Vogel, S., Neis, F., Brucker, S., Gawaz, M., Borst, O., Lang, F., 2014. Dynamic adhesion of eryptotic erythrocytes to immobilized platelets via platelet phosphatidylserine receptors. Am. J. Physiol. Cell Physiol. 306, C291–C297.
Wang, C., Yu, Z., Shi, X., Tang, X., Wang, Y., Wang, X., An, Y., Li, S., Li, Y., Luan, W., Chen, Z., Liu, M., Yu, L., 2018. Triclosan enhances the clearing of pathogenic intracellular Salmonella or Candida albicans but disturbs the intestinal microbiota through mTOR-independent autophagy. Frontiers in cellular and infection microbiology 8, 49.
Wang, Y., Kuhajda, F.P., Li, J.N., Pizer, E.S., Han, W.F., Sokoll, L.J., Chan, D.W., 2001. Fatty acid synthase (FAS) expression in human breast cancer cell culture supernatants and in breast cancer patients. Cancer Lett. 167, 99–104.
Weatherly, L.M., Gosse, J.A., 2017. Triclosan exposure, transformation, and human health effects. J. Toxicol. Environ. Health B Crit. Rev. 20, 447–469.
Weinlich, R., Oberst, A., Beere, H.M., Green, D.R., 2017. Necroptosis in development, inflammation and disease. Nat. Rev. Mol. Cell Biol. 18, 127–136.
Winitthana, T., Lawanprasert, S., Chanvorachote, P., 2014. Triclosan potentiates epithelial-to-mesenchymal transition in anoikis-resistant human lung cancer cells. PLoS One 9, e110851.
Yoon, D.S., Choi, Y., Cha, D.S., Zhang, P., Choi, S.M., Alfhili, M.A., Polli, J.R., Pendergrass, D., Taki, F.A., Kapalavavi, B., Pan, X., Zhang, B., Blackwell, T.K., Lee, J.W., Lee, M.H., 2017. Triclosan disrupts SKN-1/Nrf2-mediated oxidative stress response in C. elegans and human mesenchymal stem cells. Sci. Rep. 7, 12592.
Yueh, M.F., Tukey, R.H., 2016. Triclosan: a widespread environmental toxicant with many biological effects. Annu. Rev. Pharmacol. Toxicol. 56, 251–272.
Zelenak, C., Pasham, V., Jilani, K., Tripodi, P.M., Rosaclerio, L., Pathare, G., Lupescu, A., Faggio, C., Qadri, S.M., Lang, F., 2012. Tanshinone IIA stimulates erythrocyte phosphatidylserine exposure. Cell. Physiol. Biochem.: Int. J. Exp. Cell. Physiol., Biochem, and Pharma. 30, 282–294.
Zhang, N., Wang, W., Li, W., Liu, C., Chen, Y., Yang, Q., Wang, Y., Sun, K., 2015. Inhibition of 11beta-HSD2 expression by triclosan via induction of apoptosis in human placental syncytiotrophoblasts. J. Clin. Endocrinol. Metab. 100, E542–E549.
Zhang, P., Yang, M., Zeng, L., Liu, C., 2018. P38/TRHr-Dependent regulation of TPO in thyroid cells contributes to the hypothyroidism of triclosan-treated rats. Cell. Physiol. Biochem.: Int. J. Exp. Cell. Physiol., Biochem., and Pharma. 45, 1303–1315.
Zierle, J., Bissinger, R., Bouguerra, G., Abbes, S., Lang, F., 2016. Triggering of suicidal erythrocyte death by regorafenib. Cell. Physiol. Biochem.: Int. J. Exp. Cell. Physiol., Biochem, and Pharma. 38, 160–172.